Manifolds in random media: Multifractal behavior

Yadin Y. Goldschmidt and Thomas Blum
Department of Physics and Astronomy, University of Pittsburgh, Pittsburgh, Pennsylvania 15260
(Received 10 March 1993)

The multifractal nature of the probability distribution for the head of a directed polymer in a (1+1)-dimensional disordered medium is derived analytically. This is achieved by using a mapping of the model into a corresponding "toy" model which consists of a classical particle in a combination of a harmonic potential and a long-ranged random potential. We use the solution of the latter problem that incorporates replica-symmetry breaking within the framework of a variational approximation. The results are expressed in terms of a distribution $f(\alpha)$ reminiscent of that used in dynamical systems. We compare our results with numerical simulations.

PACS: number(s) 05.40.+j, 05.20.-y, 75.10.Nr, 02.50.-r

I. INTRODUCTION

Systems subject to quenched disorder play a fundamental role in nature but are difficult to investigate analytically. Attention has recently been focused on "simple" prototypes of these systems, including manifolds in a random potential, and more specifically directed walks in random media [1–10]. Such walks are characterized by superdiffusivity ($\langle\langle x^2\rangle\rangle \sim t^{2\nu}$ with $\nu > \frac{1}{2}$), and some of their properties are known exactly in $1+1$ dimensions, for example, the value of $\nu = \frac{2}{3}$ and the exponent ω governing free-energy fluctuations. Mappings from directed polymers to the Kardar-Parisi-Zhang (KPZ) equation [11] for kinetic roughening of driven interfaces and to the randomly stirred Burger's equation [12,13] have enhanced interest in these models.

Recently, we have reported on extensive numerical simulations on the probability distribution $P_{\rm DP}(x,t)$ for the head of a directed polymer in 1+1 dimensions [10], where t indicates the distance along the directed axis and x marks the position in the transverse direction. Analysis of the results has revealed a multifractal nature of the probability distribution which can be summarized in terms of a function $f(\alpha)$ similar to that used for dynamical systems [14–21]. The probability distribution has a very broad distribution and cannot be characterized by a single exponent; rather its description requires a spectrum of exponents. The $f(\alpha)$ spectrum can be thought of as a fingerprint — it encodes a vast amount of information about a system, including both its average and typical behavior which might be vastly different.

The directed-polymer probability distribution exhibits scaling behavior in terms of the variable $u = x/t^{\frac{2}{3}}$. Furthermore, in terms of this variable, we have found that

$$P_{\rm DP}(x,t) \sim \exp\{-\alpha\lambda u^y\}, \tag{1}$$

where the exponent α is distributed for different realizations of the disorder as

$$\mathcal{P}(\alpha) = \mathcal{N}\exp\{-f(\alpha)\lambda u^y\}. \tag{2}$$

The mean probability distribution is given by Eq. (1) with $\alpha = 1$; this determines λ. The value $\alpha = 1$ corresponding to the mean distribution is generally very different from its typical value which corresponds to α_0, the position of the minimum of $f(\alpha)$. Actually, we have uncovered two different scaling regions: One for $0.25 \le u \le 1.1$ where the index y satisfies $y \simeq 2.1 \pm 0.1$ and $f(\alpha)$ has a broad distribution, and another for $u \ge 2$ where $y \simeq 3.0 \pm 0.1$ and $f(\alpha)$ becomes trivial (very narrowly distributed) for large u. In this work, we derive analytically the properties of $f(\alpha)$ in the first region and show that its universal features can be obtained from a "toy" model consisting of a classical particle in one dimension. We compare the analytic results with simulations we have carried out on both the toy model and directed polymers in $1+1$ dimensions.

Parisi [3], Mézard [4], and Bouchaud and Orland [5] have shown that under certain assumptions, one can map the directed-polymer problem in $1+1$ dimensions onto a simpler toy model. This mapping can account for many (though not all) of the properties of directed polymers. The toy model [22,23] involves a classical particle in a one-dimensional potential consisting of a harmonic part and a spatially correlated random part. Its Hamiltonian is given by

$$H = \frac{\mu}{2}\omega^2 + V(\omega), \tag{3}$$

where ω denotes the position of the particle and $V(\omega)$ is a random potential with a Gaussian distribution characterized by

$$\langle V(\omega)\rangle = 0, \tag{4}$$

$$\langle V(\omega)V(\omega')\rangle = -\frac{g}{2(1-\gamma)}|\omega-\omega'|^{2-2\gamma} + \text{const},$$

where the angular brackets indicate averaging over the random potential. By a Gaussian distribution, we mean:

$$P[V(\omega)] = \mathcal{N}\exp\left\{-\frac{1}{2}\int d\omega d\omega' V(\omega)\Delta(\omega-\omega')V(\omega')\right\} \tag{5}$$

with some appropriate function $\Delta(\omega)$.

We shall consider cases in which the potential has long-range correlations, (i.e., $\gamma < 1$), and as will be seen below the mapping from directed polymers requires $\gamma = \frac{1}{2}$. This means that the "price" one pays for this simplification is trading a model with no correlations (or short-range correlations) of the random potential for a model with long-range correlations of the disorder but independent of "time." Villain *et al.* [22] have studied the $\gamma = \frac{1}{2}$ case while investigating the effect of randomness on the commensurate-incommensurate transition.

II. THE MAPPING

In this section we review the mapping between the two models, mainly following Parisi's approach. We start with the directed-polymer partition function in $1+1$ which is given by

$$Z_{\mathrm{DP}} = \int dx(t)\exp\left\{-\int dt\left(\frac{\kappa}{2}\dot{x}^2 + \beta_{\mathrm{DP}}V(x(t),t)\right)\right\} \tag{6}$$

with

$$\langle V(x,t)V(x',t')\rangle = v_0^2\delta(x-x')\delta(t-t'), \tag{7}$$

where κ characterizes the stiffness of the polymer and β_{DP} the inverse temperature. This partition function sums over all configurations of a directed polymer (having no overhangs) lying on a substrate with an uncorrelated random potential. The spatial direction which always increases is denoted "time" and labeled by t; the "transverse" direction is labeled x. (When switching from a lattice description to a continuum description, κ may acquire some temperature dependence which may not be a simple function of β_{DP}.)

Now let us replicate the partition function and carry out the average over the (quenched) random potential, obtaining

$$\langle Z_{\mathrm{DP}}^n\rangle = \int\prod_\alpha [dx_\alpha(y)]\exp\left\{-\int dt\left(\frac{\kappa}{2}\sum_\alpha \dot{x}_\alpha^2 - \frac{\beta_{\mathrm{DP}}^2 v_0^2}{2}\sum_{\substack{\alpha,\beta\\(\alpha\neq\beta)}}\delta(x_\alpha(t)-x_\beta(t))\right)\right\}. \tag{8}$$

This expression looks like the Euclidean version of an n-body quantum-mechanical system with the following Hamiltonian:

$$H_n = -\frac{1}{2\kappa}\sum_\alpha\frac{\partial^2}{\partial x_\alpha^2} - \frac{\beta_{\mathrm{DP}}^2 v_0^2}{2}\sum_{\substack{\alpha,\beta\\(\alpha\neq\beta)}}\delta(x_\alpha - x_\beta). \tag{9}$$

The ground state of this Hamiltonian is [2–5]:

$$|\Psi_0\rangle = \mathcal{N}\exp\left\{\frac{-g}{2}\sum_{\substack{\alpha,\beta\\(\alpha\neq\beta)}}|x_\alpha - x_\beta|\right\}, \tag{10}$$

with

$$g = \kappa\beta_{\mathrm{DP}}^2 v_0^2/2. \tag{11}$$

Parisi [3] has suggested an approximate ansatz for the Green's function of this model; his prescription entails simply multiplying the "Bethe" wave function of Eq. (10) by a product of free Green's functions, resulting in

$$G_{\mathrm{DP}}(x_1,\ldots,x_n) = \mathcal{N}\exp\left\{-\frac{\kappa}{2t}\sum_\alpha {x_\alpha}^2 - \frac{g}{2}\sum_{\substack{\alpha,\beta\\(\alpha\neq\beta)}}|x_\alpha - x_\beta|\right\}. \tag{12}$$

Compare this expression to the analogous expression for the toy-model Green's function which can be obtained by replicating the toy-model partition function defined by Eqs. (3) and (4) and averaging it over the random potential:

$$G_{\mathrm{TM}}(\omega_1,\ldots,\omega_n) = \mathcal{N}\exp\left\{-\frac{\beta\mu}{2}\sum_\alpha\omega_\alpha^2 - \frac{g\beta^2}{4(1-\gamma)}\sum_{\substack{\alpha,\beta\\(\alpha\neq\beta)}}|\omega_\alpha-\omega_\beta|^{2-2\gamma}\right\}. \tag{13}$$

Note that they are the same when one applies the following identifications:

$$\left.\begin{matrix}\gamma\\ \mu\\ \beta\\ \omega\end{matrix}\right\} \Longleftrightarrow \begin{cases} \frac{1}{2} \\ \kappa \\ t^{\frac{1}{3}} \\ u = x/t^{\frac{2}{3}} \end{cases} . \tag{14}$$

Consequently, one sees that (subject to Parisi's approximation) the probability distributions are related through

$$\begin{aligned}\langle P_{\rm DP}(x,t)\rangle &= \lim_{n\to 0}\int dx_2\cdots dx_n G_{\rm DP}(x_1,\ldots,x_n)\\ &= \lim_{n\to 0}(t^{\frac{2}{3}})^{n-1}\int d\omega_2\cdots d\omega_n G_{\rm TM}(\omega_1,\ldots,\omega_n)\\ &= t^{-\frac{2}{3}}\langle P_{\rm TM}(u,\beta=t^{\frac{1}{3}})\rangle,\end{aligned} \tag{15}$$

where $P_{\rm TM}(u,\beta)$ is the probability distribution of the toy model for the particle to be at location u. Here β is the inverse temperature in the toy model, which has acquired a value of $t^{\frac{1}{3}}$ via the mapping. Note that for large β, the toy-model probability distribution is asymptotically independent of β, as is evident from the fact [23,24] that all the moments calculated with this probability distribution

$$\langle u^{2p}\rangle \underset{\beta\to\infty}{\sim} \text{const}\times\left(\frac{g}{\mu^2}\right)^{\frac{2p}{3}}, \tag{16}$$

approach a limit independent of β. Thus for large t,

$$\begin{aligned}\langle P_{\rm DP}(x,t)\rangle &\overset{\text{large } t}{\sim} t^{-\frac{2}{3}}P_{\rm TM}(u,\beta=\infty)\\ &= t^{-\frac{2}{3}}P_{\rm TM}\left(\frac{x}{t^{\frac{2}{3}}},\infty\right),\end{aligned} \tag{17}$$

which is the scaling we have observed from the numerical simulation of the directed polymer [10].

Note also that in the case of $\gamma = \frac{1}{2}$ the probability distribution of the random potential is given by

$$dP[V(\omega)] = [dV(\omega)]\exp\left\{-\frac{1}{2g}\int d\omega\left(\frac{\partial V}{\partial\omega}\right)^2\right\}. \tag{18}$$

This corresponds to the choice

$$\Delta(\omega-\omega') = -\frac{1}{g}\frac{d^2}{d\omega^2}\delta(\omega-\omega') \tag{19}$$

in Eq. (5). Note that here the derivative of V has an uncorrelated Gaussian distribution. The two-point average given in Eq. (4) follows simply from the fact that the associated propagator of a free particle in one (temporal) dimension scales like $|\omega|$. In practice, one can generate such a potential by summing over the steps of a random walker, whose average square displacement from the origin grows linearly with time, which corresponds here to the variable ω.

III. CALCULATION OF $f(\alpha)$: REPLICA SYMMETRIC

Much of the average behavior of directed polymers is dominated by rare events. In order to extract information about typical events as well, it is useful to study the moments of the probability distribution. Just as in the derivation of Eq. (17), one can show that

$$\langle P^q_{\rm DP}(x,t)\rangle \approx t^{-\frac{2q}{3}}\langle P^q_{\rm TM}(u,\beta=t^{\frac{1}{3}})\rangle. \tag{20}$$

Hence, we will concentrate hereafter on the calculation of the averaged $q^{\rm th}$ moment of the toy-model probability distribution. We consider the general version of the toy model with arbitrary $\gamma < 1$, even though directed polymers corresponds to $\gamma = \frac{1}{2}$.

One can express the qth moment as

$$\langle P^q_{\rm TM}(\omega,\beta)\rangle = \lim_{n\to 0}\int d\omega_{q+1}\cdots d\omega_{nq}\exp\{-\beta H(\omega_1,\ldots,\omega_{nq})\}\Big|_{\omega_1=\cdots=\omega_q=\omega}, \tag{21}$$

where

$$H(\omega_1,\ldots,\omega_{nq}) = \frac{\mu}{2}\sum_{a=1}^{nq}\omega_a^2 + \frac{g\beta}{4(1-\gamma)}\sum_{a,b}|\omega_a-\omega_b|^{2-2\gamma}. \tag{22}$$

Mézard and Parisi [24] have observed that a good approximation for the toy model can be obtained by replacing the nonharmonic part of the Hamiltonian by a quadratic one

$$H_\sigma = \frac{\mu}{2}\sum_a\omega_a^2 - \frac{1}{2}\sum_{a,b}\sigma_{ab}\omega_a\omega_b, \tag{23}$$

with the σ parameters determined by the stationarity condition of the variational free energy. (For other uses of this method see Refs. [6] and [25–28].) These conditions read

$$\sigma_{ab} = \beta\hat{g}\left(\frac{G_{aa}+G_{bb}-2G_{ab}}{\beta}\right)^{-\gamma}, \quad a\neq b \tag{24}$$

and

$$\sigma_{aa} = -\sum_{b\ (\neq a)}\sigma_{ab}, \tag{25}$$

where

$$G_{ab} = \left[(\mu-\sigma)^{-1}\right]_{ab} \tag{26}$$

and

$$\hat{g} = g\frac{\Gamma(\frac{3}{2}-\gamma)}{\Gamma(\frac{1}{2})}2^{1-\gamma}. \tag{27}$$

These equations yield a replica-symmetric solution (in-

variant under permutations of the replicas) at all temperatures, as well as a solution with broken replica symmetry below a certain temperature $1/\beta_c$. The latter solution agrees much better with the numerical value of the two-point correlation function $\langle\omega^2\rangle$ at low temperatures exhibiting the correct low-temperature scaling limit (the replica-symmetric solution yields an $\langle\omega^2\rangle$ that diverges at zero temperature). For the details of this calculation, see Ref. [24].

Here we would like to use the variational approximation represented by H_σ [Eq. (23)] to calculate the q^{th} moments of the probability distribution. We start by considering the replica-symmetric (RS) case, leaving the more technically involved replica-symmetry-breaking (RSB) solution to the next section.

For the RS case, the variation yields [24]

$$\sigma_{ab} = \begin{cases} 2^{-\gamma}\beta^{1+\gamma}\mu^\gamma\hat{g} \equiv \sigma & \text{if } a \neq b \\ -(n-1)2^{-\gamma}\beta^{1+\gamma}\mu^\gamma\hat{g} & \text{if } a = b \end{cases} . \tag{28}$$

The easiest method of calculating $\langle P^q_{\text{TM}}\rangle$ involves simply carrying out the integrations over ω_i in Eq. (21) one-by-one. Observe that

$$\int d\omega_\ell \exp\{-\beta H_\ell(\omega_1,\ldots,\omega_\ell)\}$$

$$= \mathcal{N}_{\ell-1}\exp\{-\beta H_{\ell-1}(\omega_1,\ldots,\omega_{\ell-1})\}, \tag{29}$$

with $H_{\ell-1}$ characterized by renormalized parameters $\mu_{\ell-1}$ and $\sigma_{\ell-1}$ related to μ_ℓ and σ_ℓ of H_ℓ by

$$\begin{aligned} \mu_{\ell-1} &= \lambda(\ell)\mu_\ell \\ \sigma_{\ell-1} &= \lambda(\ell)\sigma_\ell, \end{aligned} \tag{30}$$

with

$$\lambda(\ell) = \frac{\mu + \ell\sigma}{\mu + (\ell-1)\sigma}. \tag{31}$$

Using Eq. (21) with H replaced by H_σ, we find

$$\begin{aligned} \langle P^q_{\text{TM}}(\omega,\beta)\rangle &= \mathcal{N}(q)\exp\left\{-\frac{q\beta\mu_q}{2}\omega^2\right\} \\ &= \mathcal{N}(q)\exp\left\{-\frac{q\beta\mu^2}{2(\mu+q\sigma)}\omega^2\right\} \end{aligned} \tag{32}$$

with

$$\mathcal{N}(q) = \left(\frac{\beta\mu}{2\pi}\right)^{\frac{q}{2}} \frac{\mu^{\frac{1}{2}}}{(\mu+q\sigma)^{\frac{1}{2}}}, \tag{33}$$

where we have substituted

$$\mu_q = \mu\lambda(nq)\lambda(nq-1)\cdots\lambda(q+1) = \frac{\mu+nq\sigma}{\mu+q\sigma} \underset{n\to 0}{\longrightarrow} \frac{\mu^2}{\mu+q\sigma}. \tag{34}$$

Toward our goal of calculating $f(\alpha)$, we now introduce the function $\tau(q)$ (which bears some resemblance to its counterpart in dynamical systems [10,15–18]) through the definition

$$\langle P^q_{\text{TM}}(\omega,\beta)\rangle = \langle P_{\text{TM}}(\omega,\beta)\rangle^{\tau(q)}. \tag{35}$$

We find (disregarding the small correction due to the normalization constant which is negligible for sufficiently large ω):

$$\tau(q) = q\frac{\mu+\sigma}{\mu+q\sigma} = q\frac{1+\gamma^{-1}T^{-(1+\gamma)}}{1+q\gamma^{-1}T^{-(1+\gamma)}}, \tag{36}$$

where we have introduced the reduced temperature variable:

$$T = \frac{1}{\beta}\mu^{\frac{1-\gamma}{1+\gamma}}\left(\gamma 2^{-\gamma}\hat{g}\right)^{-\frac{1}{1+\gamma}}. \tag{37}$$

Note that we have analytically continued the variable q to be a real number satisfying $-\gamma T^{1+\gamma} < q < \infty$ and that $\tau(q)$ does not exist for values of $q < -\gamma T^{1+\gamma}$.

Next one obtains the multifractal spectrum $f(\alpha)$ by calculating the Legendre transform of $\tau(q)$:

$$f(\alpha) = \tau(q) - q\alpha \tag{38}$$

with $\alpha = \tau'(q)$. Using expression (36) for $\tau(q)$, we find

$$f(\alpha) = \gamma T^{1+\gamma}\left(\sqrt{\alpha} - \sqrt{1+\gamma^{-1}T^{-(1+\gamma)}}\right)^2. \tag{39}$$

Furthermore, expanding $f(\alpha)$ around its minimum ($\alpha_0 = 1+\gamma^{-1}T^{-(1+\gamma)}$) yields

$$f(\alpha) = \frac{1}{4(\alpha_0-1)\alpha_0}(\alpha-\alpha_0)^2. \tag{40}$$

Mézard and Parisi [24] have found that the RS solution is good for $T > 1$ but for lower T it should be replaced by the RSB solution. Since we are interested in the long-"time" behavior of directed polymers, we desire the low-T behavior of the toy model (as $T \propto t^{-\frac{1}{3}}$). If we nevertheless take the RS result at low T, we find $\alpha_0 \sim T^{-\frac{3}{2}}$ for $\gamma = \frac{1}{2}$ which does not agree with our numerical simulations for the directed polymer where we have observed $\alpha_0 \sim T^{-1}$. (See the discussion in Sec. V.) We will see in the next section that the correct scaling at low temperature is obtained from the RSB solution.

IV. CALCULATION OF $f(\alpha)$ REPLICA-SYMMETRY BREAKING

In order to derive the result for the case of RSB, we reformulate the problem in the following way: Within the framework of the variational approximation, we consider

$$\begin{aligned} \langle P^q_{\text{TM}}(\omega,\beta)\rangle &= \int\prod_{a=1}^{nq} d\omega_a \delta(\omega_1-\omega)\cdots\delta(\omega_q-\omega)\exp\left\{-\frac{\beta\mu}{2}\sum_a\omega_a^2 + \frac{\beta}{2}\sum_{a,b}\sigma_{ab}\omega_a\omega_b\right\} \\ &= \int\frac{dk_1}{2\pi}\cdots\frac{dk_q}{2\pi}\exp\left\{i\sum_{a=1}^{nq}k_a\omega_a^0\right\}\int\prod_{a=1}^{nq}d\omega_a\exp\left\{-\frac{\beta}{2}\sum_a(\mu\delta_{ab}-\sigma_{ab})\omega_a\omega_b - i\sum_{a=1}^{nq}k_a\omega_a\right\}, \end{aligned} \tag{41}$$

where

$$\mathbf{k} = (k_1, \ldots, k_q, 0, \ldots, 0),$$
$$\boldsymbol{\omega}^0 = (\omega, \ldots, \omega, 0, \ldots, 0) \tag{42}$$

are vectors of length nq, and the limit $n \to 0$ must eventually be taken.

Recall that G_{ab} is defined:

$$G_{ab} = (\mu I - \sigma)^{-1}_{ab}, \quad a, b = 1, \ldots, nq; \tag{43}$$

now let us denote by $\hat{G}$ the following $q \times q$ submatrix of G:

$$\hat{G}_{ab} = G_{ab}, \quad a, b = 1, \ldots, q. \tag{44}$$

We then find

$$\begin{aligned}\langle P^q_{\mathrm{TM}} \rangle &= \left(\frac{2\pi}{\beta}\right)^{\frac{nq}{2}} (\det G)^{\frac{1}{2}} \int \prod_{i=1}^{q} \left(\frac{dk_i}{2\pi}\right) \exp\left\{ i \sum_{a=1}^{q} k_a \omega_a^0 - \frac{1}{2\beta} \sum_{a,b=1}^{q} k_a \hat{G}_{ab} k_b \right\} \\ &= \left(\frac{2\pi}{\beta}\right)^{\frac{q(n-1)}{2}} (\det \hat{G})^{-\frac{1}{2}} (\mathrm{Det} G)^{\frac{1}{2}} \exp\left\{ -\frac{\beta}{2} \sum_{a,b=1}^{q} \hat{G}^{-1}_{ab} \omega_a^0 \omega_b^0 \right\} \\ &= \left(\frac{\beta}{2\pi}\right)^{\frac{q}{2}} (\det \hat{G})^{-\frac{1}{2}} \exp\left\{ -\frac{\beta}{2} \left(\sum_{a,b=1}^{q} \hat{G}^{-1}_{ab} \right) \omega^2 \right\},\end{aligned} \tag{45}$$

where the limit $n \to 0$ has been taken in the last line.

For the RS solution, this result coincides with that obtained by the previous method. We note that for the RSB case this expression is not exact, rather it provides the leading contribution for sufficiently large ω. It is not exact because the permutation symmetry is broken. One should sum over all choices of the singled-out variables $1, \ldots, q$ and then divide by the number of such choices; more explicitly, one should make the replacement:

$$\delta(\omega_1 - \omega) \cdots \delta(\omega_q - \omega) \longrightarrow \frac{\Gamma(nq - q + 1)\Gamma(q+1)}{\Gamma(nq+1)} \sum_{(i_1, \cdots, i_q)} \delta(\omega_{i_1} - \omega) \cdots \delta(\omega_{i_q} - \omega) \tag{46}$$

in Eq. (41) where $(i_1, \ldots, i_q)$ indicate any q distinct integers between 1 and nq. For technical reasons it is too difficult to obtain explicit results for general q and a matrix σ with infinite-step RSB. However, by considering different cases, we have been able to verify that the choice made in Eq. (41), i.e., having the q values grouped together in the left-hand corner of G, gives the dominant contribution for large ω^2. This is due to the ultrametric structure of the matrix σ and the fact that in the Parisi scheme $G(x)$ is a monotonic function [29]. (See the Appendix.)

To calculate $\tau(q)$, we must evaluate the coefficient of $-\omega^2$ in Eq. (45):

$$a(q) = \frac{\beta}{2} \sum_{a,b=1}^{q} \hat{G}^{-1}_{ab}. \tag{47}$$

Then in terms of this function, $\tau(q)$ is

$$\tau(q) = \frac{a(q)}{a(1)} \tag{48}$$

(again ignoring the contribution due to the normalizing factor). Since $\hat{G}$ is also a hierarchical matrix, it has an eigenvector of the form $(1, \ldots, 1)$ with an associated eigenvalue $\tilde{\lambda}$. It then follows that

$$a(q) = \frac{\beta q}{2} \left[\tilde{\lambda}(q)\right]^{-1}. \tag{49}$$

For the case of infinite-step RSB, the matrix $G = (\mu I - \sigma)^{-1}$ is represented by the pair $(\tilde{G}, G(x))$, which can in turn be obtained from $(\tilde{\sigma}, \sigma(x))$ which is a solution of the stationarity conditions, Eqs. (24) and (25). Mézard and Parisi [24] have supplied $(\tilde{\sigma}, \sigma(x))$. However, two misprints occur in the expressions in their paper; they are corrected below:

$$\sigma(x) = \begin{cases} \frac{\mu}{\gamma} T^{-1}, & 0 < x < x_1 \\ \left(\frac{1+\gamma}{2\gamma}\right) A x^{\frac{2\gamma}{1-\gamma}}, & x_1 < x < x_2 \\ \left(\frac{1+\gamma}{2\gamma}\right) A x_2^{\frac{2\gamma}{1-\gamma}}, & x_2 < x < 1, \end{cases} \tag{50}$$

$$\tilde{\sigma} = \int_0^1 dx \sigma(x), \tag{51}$$

where

$$A = \mu(x_1)^{-\frac{1+\gamma}{1-\gamma}}, \quad x_1 = \frac{1+\gamma}{2} T, \quad \text{and } x_2 = \frac{1+\gamma}{2}. \tag{52}$$

Using this solution, we calculate G [using Eqs. (AII.6) and (AII.7) of Ref. [6] for inverting a hierarchical matrix]; we find

$$\tilde{G} = \frac{1+\gamma}{\mu\gamma} T^{-1}, \tag{53}$$

$$G(x) = \begin{cases} \frac{1}{\mu T}\left(\frac{1}{\gamma}\right), & 0 < x < x_1 \\ \frac{1}{\mu T}\left[\frac{1+\gamma}{\gamma} - \left(\frac{x}{x_1}\right)^{-\frac{2}{1-\gamma}}\right], & x_1 < x < x_2 \\ \frac{1}{\mu T}\left[\frac{1+\gamma}{\gamma} - \left(\frac{x_2}{x_1}\right)^{-\frac{2}{1-\gamma}}\right], & x_2 < x < 1. \end{cases} \tag{54}$$

The eigenvalue $\tilde{\lambda}$ of $\hat{G}$, the $q \times q$ submatrix of G, is given by (see the Appendix of Ref. [28])

$$\tilde{\lambda} = \tilde{G} - \int_q^1 G(x)dx. \tag{55}$$

Let us restrict our attention to the region $0 < q < 1$ for now. In that case, we find

$$\tilde{\lambda}(q) = \begin{cases} \frac{1}{\mu} + \frac{q}{\mu\gamma T}, & 0 < q < x_1 \\ \frac{q}{\mu T}\left[\frac{1+\gamma}{\gamma} + \frac{1-\gamma}{1+\gamma}\left(\frac{q}{x_1}\right)^{-\frac{2}{1-\gamma}}\right], & x_1 < q < x_2 \\ \frac{q}{\mu T}\left(\frac{1+\gamma}{\gamma}\right) + \frac{1-q}{\mu T}\left(\frac{x_2}{x_1}\right)^{-\frac{2}{1-\gamma}}, & x_2 < q < 1. \end{cases} \tag{56}$$

Then using $\tau(q) = q\tilde{\lambda}(1)/\tilde{\lambda}(q)$, we finally obtain

$$\tau(q) = \begin{cases} \frac{q(1+\gamma)}{\gamma T + q}, & 0 < q < \frac{1+\gamma}{2}T \\ \left[1 + \frac{\gamma(1-\gamma)}{(1+\gamma)^2}\left(\frac{(1+\gamma)T}{2q}\right)^{\frac{2}{1-\gamma}}\right]^{-1}, & \frac{1+\gamma}{2}T < q < \frac{1+\gamma}{2} \\ \left[1 + \frac{\gamma(1-q)}{q(1+\gamma)}T^{\frac{2}{1-\gamma}}\right]^{-1}, & \frac{1+\gamma}{2} < q < 1. \end{cases} \tag{57}$$

We will now use the following analytic continuation to define $\tau(q)$ outside the range $0 < q < 1$: for $q > 1$ we continue to use the expression for $q > \frac{1+\gamma}{2}$, and for $q < 0$, we use the expression for $q < \frac{1+\gamma}{2}T$. Notice also that for negative q, $\tau(q)$ is defined only for $q > -\gamma T$. Explicit calculations for $q = 2$ and negative q have confirmed this analytic continuation (for large ω^2). (See the Appendix.) Expression (57) for $\tau(q)$ is valid for $T < 1$ where the RSB solution exists. For $T > 1$ one has to use the RS result, Eq. (36), which coincides with Eq. (57) for $T = 1$.

In Fig. 1 we show a graph of $\tau(q)$ for $\gamma = \frac{1}{2}$ and $T = 0.5$, and compare it with the RS result. Figure 2 depicts the corresponding $f(\alpha)$ obtained as a Legendre transform of $\tau(q)$. In the vicinity of α_0, where $f(\alpha)$ aquires its minimum, we would like to show the analytic expression. Since α_0 is the slope of $\tau(q)$ at $q = 0$, we use the expression for $\tau(q)$ in the region $q < \frac{1+\gamma}{2}T$. We find that in this region, its Legendre transform is given by

$$f(\alpha) = \gamma T\left(\sqrt{\alpha} - \sqrt{\frac{1+\gamma}{\gamma T}}\right)^2. \tag{58}$$

Thus for α near $\alpha_0 = \frac{1+\gamma}{\gamma T}$ we have

$$f(\alpha) \approx \frac{1+\gamma}{4}\left(\frac{\gamma T}{1+\gamma}\alpha - 1\right)^2. \tag{59}$$

From this result, we see that $f(\frac{\alpha}{T})$ is independent of T as found in our numerical simulations. This result, valid for small T ($T < 1$) is to be contrasted with the RS result, which if continued to small T (where it is not the correct solution) implies that $f(\frac{\alpha}{T^{1+\gamma}})$ is independent of T in disagreement with our simulations. This is another proof for the usefulness of the RSB solution.

One of the predictions arising from these calculations is that $\langle P^q_{\rm TM}(\omega)\rangle$ diverges for some finite q ($q = -\gamma T$ in the RSB calculation). What is the physical implication of this result if it is a genuine property of the toy model? It provides some information on the sample-to-sample distribution of probabilities. Let $h[P_{\rm TM}(\omega)]$ be the sample-to-sample distribution of probabilities at ω, so that

$$\int_0^1 h[P_{\rm TM}(\omega)]P^q_{\rm TM}(\omega)dP_{\rm TM}(\omega) = \langle P^q_{\rm TM}(\omega)\rangle. \tag{60}$$

The divergence of $\langle P^q_{\rm TM}\rangle$ at a finite, nonzero q indicates

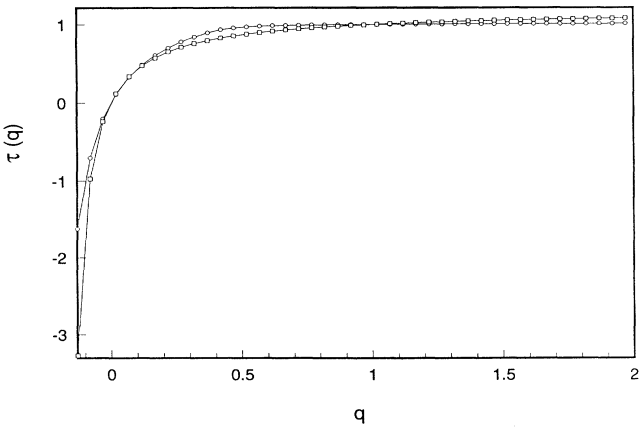

FIG. 1. The function $\tau(q)$ derived from the variational approach to the toy model. The □'s indicate the RS solution, and ○'s indicate the RSB solution.

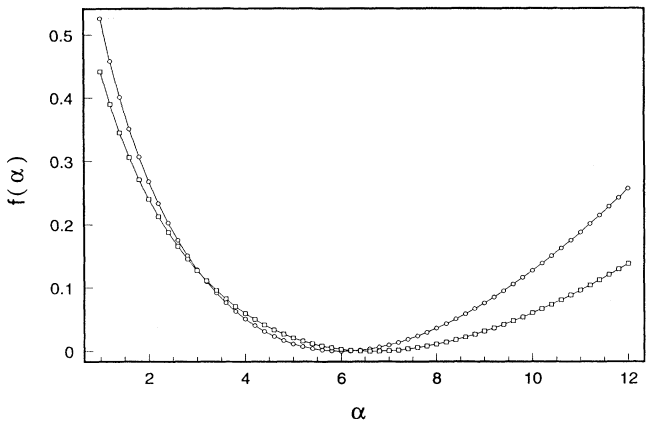

FIG. 2. The corresponding $f(\alpha)$ spectra, i.e., the Legendre transform of $\tau(q)$.

(1) that there is no minimal P (other than zero) since $\langle P_{\rm TM}^q \rangle$ would not diverge in such a case; and (2) that $h[P]$ vanishes at $P = 0$, since $\langle P_{\rm TM}^q \rangle$ would diverge at $q < 0$ if that were the case. If one assumes that $h[P]$ has a power-law distribution at small P, the divergence of $\langle P_{\rm TM}^q(\omega) \rangle$ for $q < -\gamma T$ would imply

$$\lim_{P \to 0} h[P] \propto P^{-1+\gamma T}. \tag{61}$$

This prediction requires further numerical testing since it relies on rare events.

V. SIMULATIONS

We have recently reported on the simulations of (1+1)-dimensional directed polymers (for t up to 1000) on a disordered substrate, from which we have extracted the average probability distribution and its moments [10]. As mentioned in the Introduction, that investigation has revealed that the universal part of $P_{\rm DP}(x,t)$ scales as $P_{\rm DP} \propto \exp\{-\alpha \lambda u^y\}$, where the exponent α is distributed for different samples according to $\mathcal{P}(\alpha) \propto \exp\{-f(\alpha)\lambda u^y\}$. Furthermore, two scaling regimes were found: the first ($0.25 \leq u < 1.1$) has $y = 2.1 \pm 0.1$ and a broadly distributed $f(\alpha)$; and the second ($u > 2$) has $y = 3.0 \pm 0.1$ and an increasingly narrowly distributed $f(\alpha)$ as u grows large. In the inner (nearly Gaussian) region, the numerical data furnishes an $f(\alpha)$, which is nearly independent of u. In addition, at low temperatures we have found that the position of its minimum, α_0, scales with time as $\alpha_0 \propto t^{0.3}$ and with reciprocal temperature as $\alpha_0 \propto \beta_{\rm DP}$. Let us compare this behavior with the results found in the previous sections. We have seen above that the toy-model calculations using the RS variational approximation yield at low T, $\alpha_0 \propto T^{-3/2}$ (for $\gamma = \frac{1}{2}$), while those using the RSB solution lead to $\alpha_0 \propto T^{-1}$. From the mapping between directed polymers to the toy model [Eq. (14)] and the expression (37) for T, we obtain

$$T^{-1} \propto \kappa^{1/3} \beta_{\rm DP}^{4/3} t^{1/3}. \tag{62}$$

Note then that the RSB solution provides the correct time dependence. The scaling with $\beta_{\rm DP}$ is more subtle since when switching from a lattice model (used for the simulations) to a continuum model (used for the calculations), κ acquires some nontrivial temperature dependence. But even when the temperature dependence of κ is ignored, the RSB solution agrees more closely with observation.

In order to test the analytic results directly without relying on the mapping between the two models, we have also simulated the toy model directly at finite temperature, extracting again the average probability distribution and its moments. We have studied a lattice version of the toy model with $\gamma = \frac{1}{2}$ and with the parameters β, μ, and g chosen to facilitate comparison with our previous directed-polymer simulations. A suitable interval of the particle's position ω (e.g., $-4 < \omega < 4$) is divided into 5000 lattice sites. For a given realization, the algorithm generates an independent random number for each site r_i; it then generates V_j, the correlated random potential at site j, by summing the random numbers in the following way:

$$V_j \propto \sum_i \mathrm{sgn}(i-j) r_i. \tag{63}$$

The quadratic term of the Hamiltonian is added to this random potential, and then the partition function and probability distribution are calculated. We have generated 50 000 realizations of 50 different moments of the probability distribution $\langle P_{\rm TM}^q(\omega, \beta) \rangle$ for $-2.0 \leq q \leq 3.0$ to determine $\tau(q)$.

The toy-model simulations reveal that as found for directed polymers the averaged probability distribution $P_{\rm TM}(\omega)$ has two scaling regimes. (See Fig. 3.) The averaged probability distribution scales in the same way as it does for directed polymers in both regions: $\sim \exp\{-\lambda_1 u^2\}$ and $\sim \exp\{-\lambda_2 u^3\}$, in the inner and outer regions, respectively. The scaling in the outer region agrees with the predictions of Villain *et al.* [22]. We have checked also for the dependence of α_0 on T^{-1} for values of T^{-1} between 4 and 20 and obtained a nearly linear dependence (a power of ~ 1.14 by a fit to five points).

VI. DISCUSSION

The mapping from (1 + 1)-dimensional directed polymers to the toy model is successful on several counts. In addition to accurately predicting the large-u scaling of the probability distribution, it yields the correct t dependence of $\langle x^2(t) \rangle$ and $\langle x^2(t) \rangle - \langle x(t) \rangle^2$ as well as higher moments and cumulants. However, one should note that it cannot be expected to reproduce every feature of directed polymers. In fact, as Mézard [4] has already pointed out, the mapping predicts

$$\langle \{\ln [P_{\rm DP}(x,t)] - \ln [P_{\rm DP}(0,t)]\}^2 \rangle - \langle \ln [P_{\rm DP}(x,t)] - \ln [P_{\rm DP}(0,t)] \rangle^2 \propto |x|, \tag{64}$$

but this behavior is seen only for small $|x|$; it saturates for larger values of $|x|$.

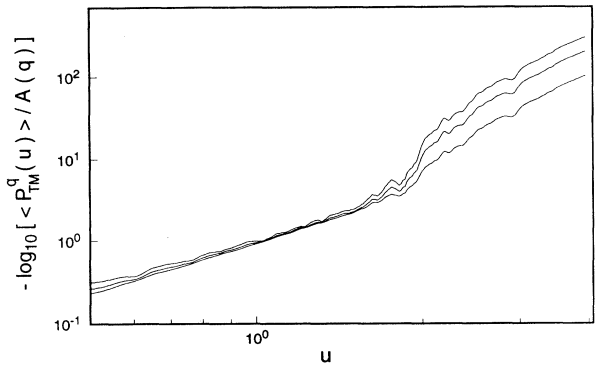

FIG. 3. A log-log plot of $\{-\log_{10}[\langle P^q_{\rm TM}(u)\rangle/A(q)]\}$ vs u, where $A(q) = \max[\langle P^q_{\rm TM}(u)\rangle]$ for $\beta = 10.0$, $\mu = 2.2$, and $g = 4.6$ for $q = 1$, 2, and 3.

Nevertheless, we have demonstrated in this paper how more of the universal features (especially the multifractal behavior) of the directed-polymer problem can be deduced from the toy model. The analytical results employ a recently introduced variational scheme that allows for replica-symmetry breaking. We have used it to calculate moments of the probability distribution. Note that this analysis only applies to the inner scaling regime of the probability distribution where u is not too large. In that region the directed-polymer distribution behaves roughly like $\exp\{-\lambda_1 u^2\}$ and is therefore consistent with the Gaussian form obtained from the Gaussian variational scheme.

We have tested the predictions that have emerged concerning the scaling properties of $f(\alpha)$. The mapping requires that toy model be examined at low temperature, where the variational procedure yields both a solution maintaining replica symmetry and a solution with infinite-step replica-symmetry breaking. We have found that the latter reproduces more accurately the scaling behavior of the $f(\alpha)$ spectrum than does the former.

For larger values of u, our simulations have revealed a behavior like $\exp\{-\lambda_2 u^3\}$. This is still consistent with the toy-model probability distribution in the tail region as discussed by Villain *et al.* [22], but it cannot be derived from the variational approximation to the toy model which yields a Gaussian form for the probability distribution. In the tail region, we have found from simulations that the function $f(\alpha)$ becomes trivial for large u, so the situation is simpler.

ACKNOWLEDGMENTS

This work was supported by the National Science Foundation under Grant No. DMR-9016907.

APPENDIX A

In this appendix we provide arguments to support our claim that in the case of RSB, the permutation taken in Eq. (41) yields the leading contribution to the averaged qth moment of the probability distribution. Although we do not have a general proof, we show how it holds for several specific examples.

First let us consider the case in which G is characterized by a one-step replica-symmetry breaking. (One-step RSB can be viewed as an approximation to infinite-step breaking.) In this case, one can express the matrix indices $a = 1, \ldots, n$ as pairs (k, γ) with $a = m(k-1) + \gamma$ where $k = 1, \ldots, \frac{n}{m}$ and $\gamma = 1, \ldots, m$ and then parametrize G in the following way:

$$G_{k,\gamma;k',\gamma'} = \begin{cases} \tilde{g} & \text{if } k = k' \text{ and } \gamma = \gamma' \\ g_1 & \text{if } k = k' \text{ and } \gamma \neq \gamma' \\ g_0 & \text{if } k \neq k'. \end{cases} \tag{A1}$$

(Note that we have relabeled nq by n since $n \to 0$ at the end.) Now one must choose q indices from the n possible values and consider $\hat{G}$, the corresponding $q \times q$ submatrix of G. Notice that before the $n \to 0$ limit one has $1 \leq m \leq n$ and one must distinguish between two cases: (1) $1 \leq q \leq m \leq n$ and (2) $1 \leq m \leq q \leq n$.

We now assume that the chosen q indices are distributed equally among q/p groups such that there are p indices in each group. Clearly, this is not the most general case; we were able to analyze the most general case only for $g_0 = 0$; see below. The $q \times q$ matrix $\hat{G}$ thus contains q/p blocks along the diagonal of size $p \times p$ each. The value of the matrix elements within these blocks is g_1 (except along the diagonal), and the value outside these blocks is g_0. Along the diagonal the value is $\tilde{g}$. That is, $\hat{G}$ has the same form as G in Eq. (A1) with $n \to q$ and $m \to p$. The eigenvalue $\tilde{\lambda}$ associated with this matrix $\hat{G}$ is

$$\tilde{\lambda} = \tilde{g} + (p-1)g_1 + (q-p)g_0, \tag{A2}$$

and hence the contribution from the permutations characterized by this choice is

$$\langle P^q(\omega)\rangle \sim \exp\left\{-\frac{\beta q \tilde{\lambda}^{-1}}{2}\omega^2\right\} \tag{A3}$$

with

$$q\tilde{\lambda}^{-1} = \frac{q}{\tilde{g} - g_1 + qg_0 + p(g_1 - g_0)}. \tag{A4}$$

Since $g_1 > g_0$ [which is a general property of $G(x)$ since it increases monotonically with x], we see that for case (1) above the minimum of $q\tilde{\lambda}^{-1}$ is obtained for $p = q$, and for case (2) it is obtained for $p = m$, which corresponds to having the largest number of indices come from the same group. As $n \to 0$, case (1) becomes $0 \leq m \leq q \leq 1$ and case (2) becomes $0 \leq q \leq m \leq 1$. So we find

$$q\tilde{\lambda}^{-1} = \begin{cases} \frac{q}{\tilde{g}+(q-1)g_1}, & m \leq q \\ \frac{q}{\tilde{g}+(m-1)g_1+(q-m)g_0}, & q \leq m, \end{cases} \tag{A5}$$

but this is exactly what one obtains from the expression

$$\tilde{\lambda} = \tilde{g} - \int_q^1 g(x)dx \tag{A6}$$

with

$$g(x) = \begin{cases} g_0, & x \le m \\ g_1, & m \le x, \end{cases} \tag{A7}$$

which has been used in Sec. IV, where all the q indices are grouped together in the upper left corner of G. Thus, this choice supplies the largest contribution for large ω, at least among permutations with equal divisions of q indices among different groups.

To consider a more general division, consider the case $g_0 = 0$. In that case the matrix $\hat{G}$ consists of unequal blocks of size $q_1, q_2, \ldots, q_\ell$ with $q = \sum_i q_i$ and $q_i \le m$, where all elements of each block have the value g_1 except for the value $\tilde{g}$ on the diagonal. Outside the blocks all elements vanish. The inverse of this matrix $\hat{G}$ can be calculated exactly. (It is no longer a Parisi-type hierarchical matrix since groups are not of equal size.) One then adds up all elements of the matrix to find their sum S [see Eq. (45)]

$$S = \sum_i \frac{q_i}{\tilde{g} + (q_i - 1)g_1}. \tag{A8}$$

For $1 \le q \le m \le n$ it is clear that the minimum value of the sum is obtained for one group of size q:

$$S = \frac{q}{\tilde{g} + (q-1)g_1} = \sum_i \frac{q_i}{\tilde{g} + (q-1)g_1}, \tag{A9}$$

which is evidently smaller than Eq. (A8) since all $q_i < q$. For the case $1 \le m \le q \le n$ one has to take q to be some multiple of m and then since $q_i \le m$ the minimum is obtained when all $q_i = m$, $i = 1, \ldots, \frac{q}{m}$ and thus

$$S = \frac{q}{\tilde{g} + (m-1)g_1}. \tag{A10}$$

As $n \to 0$ this is exactly what has been claimed.

So far the discussion has been confined to $0 \le q \le 1$. To show the analytic continuation of this formalism for q outside this region, we consider the case of $q = 2$ with infinite-step RSB. For this case the result can be obtained similarly to the calculation of Mézard and Parisi [6], who considered the average $\langle P(\omega)P(\omega')\rangle$ by putting $\omega = \omega'$. Although their result (AIII.7)is correct for one-step RSB, there is unfortunately a misprint in formula (VI.17) for the general case which should read

$$\langle P(\omega)P(\omega')\rangle = \frac{\beta}{2\pi}\int_0^1 \frac{dx}{\sqrt{\tilde{g}^2 - g^2(x)}} \times \exp\left\{-\frac{\beta}{2}\frac{\tilde{g}(\omega^2 + \omega'^2) - 2g(x)\omega\omega'}{\tilde{g}^2 - g^2(x)}\right\}, \tag{A11}$$

where we use $\tilde{g}$ and $g(x)$ instead of their $\tilde{q}$ and $q(u)$ and have also added the inverse temperature variable β. Next putting $\omega = \omega'$, we obtain

$$\langle P^2(\omega)\rangle = \frac{\beta}{2\pi}\int_0^1 \frac{dx}{\sqrt{\tilde{g}^2 - g^2(x)}} \exp\left\{-\beta\frac{\omega^2}{\tilde{g} + g(x)}\right\} \tag{A12}$$

and the leading contribution for large ω is

$$\langle P^2(\omega)\rangle \approx \exp\left\{-\beta\frac{\omega^2}{\tilde{g} + g(1)}\right\}, \tag{A13}$$

but

$$\frac{\beta}{\tilde{g} + g(1)} = \frac{\beta}{2}\frac{2}{\tilde{\lambda}(2)} = \frac{\beta\mu}{2\left(\frac{1+\gamma}{\gamma}\right)T^{-1} - T^{\frac{1+\gamma}{1-\gamma}}}, \tag{A14}$$

and thus this is exactly the result for $q = 2$ as obtained in Sec. IV showing that for $q = 2$ and infinite-step RSB our scheme gives the correct answer. We have demonstrated our claim for a few different cases; the reader is challenged to find a more general proof.

[1] D.A. Huse and C.L. Henley, Phys. Rev. Lett. **54**, 2708 (1985); D.A. Huse, C.L. Henley, and D.S. Fisher, *ibid.* **55**, 2924 (1985).

[2] M. Kardar, Phys. Rev. Lett. **55**, 2923 (1985); Nucl. Phys. **B290**, 582 (1987).

[3] G. Parisi, J. Phys. (France) **51**, 1595 (1990).

[4] M. Mézard, J. Phys. (France) **51**, 1831 (1990).

[5] J.P. Bouchaud and H. Orland, J. Stat. Phys. **61**, 877 (1990).

[6] M. Mézard and G. Parisi, J. Phys. A **23**, L1229 (1990); J. Phys. I (France) **1**, 809 (1991).

[7] T. Halpin-Healy, Phys. Rev. A **44**, R3415 (1991).

[8] D.S. Fisher and D.A. Huse, Phys. Rev. B **43**, 10728 (1991).

[9] J.M. Kim, M.A. Moore, and A.J. Bray, Phys. Rev. A **44**, 2345 (1991).

[10] Y.Y. Goldschmidt and T. Blum, Phys. Rev. E **47**, R2979 (1993).

[11] M. Kardar, G. Parisi, and Y.C. Zhang, Phys. Rev. Lett. **56**, 889 (1986).

[12] D. Forster, D.R. Nelson and M.J. Stephen, Phys. Rev. A **16**, 732 (1977).

[13] E. Medina, T. Hwa, M. Kardar, and Y.C. Zhang, Phys. Rev. A **39**, 3053 (1989).

[14] B.B. Mandelbrot, J. Fluid Mech. **62**, 331 (1974); U. Frisch and G. Parisi, in *Turbulence and Predictability in Geophysical Fluid Dynamics and Climate Dynamics*, Proceedings of the International School of Physics, "Enrico Fermi," Course LXXXVIII, Varenna, Italy, 1983, edited by M. Ghil *et al.* (North Holland, Amsterdam, 1985).

[15] T.C. Halsey, M.H. Jensen, L.P. Kadanoff, I. Procaccia, and B.I. Shraiman, Phys. Rev. A **33**, 1141 (1986).

[16] *Fractals and Disordered Systems*, edited by A. Bunde and S. Havlin (Springer-Verlag, New York, 1991).

[17] J. Feder, *Fractals* (Plenum, New York, 1988).

[18] A.W.W. Ludwig, Nucl. Phys. **B330**, 639 (1990).

[19] M. Araujo, S. Havlin, and H.E. Stanley, Phys. Rev. A **44**, 6913 (1991).

[20] A. Bunde, H.E. Roman, S. Russ, A. Aharony, and A.B. Harris, Phys. Rev. Lett. **69**, 3189 (1992).

[21] J.P. Bouchaud, D. Touati, and D. Sornette, Phys. Rev.

Lett. **68**, 1787 (1992).
[22] J. Villain, B. Semeria, F. Lançon and L. Billard, J. Phys. C **16**, 6153 (1983).
[23] U. Schulz, J. Villain, E. Brézin and H. Orland, J. Stat. Phys. **51**, 1 (1988).
[24] M. Mézard and G. Parisi, J. Phys. I (France) **2**, 2231 (1992).
[25] E.I. Shakhnovich and A.M. Gutin, J. Phys. A **22**, 1647 (1989).
[26] J.P. Bouchaud and A. Georges, Phys. Rev. Lett. **68**, 3908 (1992).
[27] Y.Y. Goldschmidt and T. Blum, J. Phys. I (France) **2**, 1607 (1992).
[28] T. Blum and Y.Y. Goldschmidt, J. Phys. A **25**, 6517 (1992).
[29] M. Mézard, G. Parisi, and M.A. Virasoro, *Spin Glass Theory and Beyond* (World Scientific, Singapore, 1987).